PHYSICAL REVIEW B **72**, 100404(R) (2005)

Characteristic Bose-Einstein condensation scaling close to a quantum critical point in $BaCuSi_2O_6$

S. E. Sebastian,[1] P. A. Sharma,[2] M. Jaime,[2] N. Harrison,[2] V. Correa,[2] L. Balicas,[3] N. Kawashima,[4] C. D. Batista,[5] and I. R. Fisher[1]

[1]*Geballe Laboratory for Advanced Materials and Department of Applied Physics, Stanford University, Stanford, California 94305, USA*

[2]*MST-NHMFL, Los Alamos National Laboratory, Los Alamos, New Mexico 87545, USA*

[3]*National High Magnetic Field Laboratory, Tallahassee, Florida 32310, USA*

[4]*Institute for Solid State Physics, University of Tokyo, Kashiwa, Chiba 277-8581, Japan*

[5]*Theoretical Division, Los Alamos National Laboratory, Los Alamos, New Mexico 87545, USA*

(Received 5 August 2005; published 30 September 2005)

We report an experimental determination of the phase boundary approaching the quantum critical point separating a quantum paramagnetic state and the proposed spin Bose-Einstein condensate of triplons in the spin dimer compound $BaCuSi_2O_6$. The ordering temperature is related to the proximity to a quantum critical point at the lower critical magnetic field $H_{c1}=23.52\pm0.03$ T by a power law parametrized by critical exponent ν. We obtain an experimental estimate of $\nu=0.63\pm0.03$ down to a temperature of 0.61 K, which is in good agreement with the mean-field prediction of $\nu=2/3$ for the three-dimensional Bose-Einstein condensation universality class.

DOI: 10.1103/PhysRevB.72.100404 PACS number(s): 75.40.−s, 75.30.−m, 75.45.+j, 75.50.−y

The class of spin dimer compounds, including $BaCuSi_2O_6$,[1,2] $TlCuCl_3$,[3–7] and $Sr_2Cu(BO_3)_2$,[8] have a singlet ground state in zero magnetic field with a gap to the lowest excited triplet state. The spin gap can be closed by an applied magnetic field, such that a quantum critical point (QCP) at a magnetic field H_{c1} separates the quantum paramagnetic state from a state characterized by long-range magnetic order. The order parameter for this transition is $\langle b^\dagger\rangle \propto M_{st}^x + iM_{st}^y$, where $\langle b^\dagger\rangle$ is the creation operator for a triplet state, and M_{st}^x and M_{st}^y are the x and y components of the staggered magnetization in the plane perpendicular to the applied field. In the limit of weak interdimer exchange coupling, the system may be described as an interacting gas of hardcore bosons, with kinetic energy and potential energy provided by the Heisenberg and Ising components of the interdimer exchange, respectively. In the absence of U(1) rotational symmetry-breaking anisotropy, the ordering transition may be interpreted as a Bose-Einstein condensation (BEC) of triplons.[9] The applied magnetic field functions as a chemical potential for the triplons, and thereby provides a convenient means to tune the BEC to criticality at the QCP.

$BaCuSi_2O_6$ has a simple and well-characterized quasi-two-dimensional structure[1,2,10] consisting of vertical Cu^{2+} dimers in a square lattice arrangement on each layer, and staggered between vertical layers. The intradimer, interdimer, and interlayer exchange couplings have been estimated from high field magnetization data[1] to be $J=4.45$ meV, $J'\simeq 0.58$ meV, $J''\simeq 0.116$ meV, respectively.[1,2] The exchange couplings in the lattice are clearly identifiable, and the small ratio of interdimer to intradimer coupling J'/J places the compound well into the strong-coupling limit, such that it is well described by the effective Hamiltonian in Ref. 1. In addition, the simple arrangement of spins on each layer in a square lattice connected only by vertical and horizontal rungs, and coupled between layers, indicates a U(1) rotationally spin symmetric Hamiltonian, which makes this a prototypical system to study the triplet analog of BEC, for which U(1) symmetry is a prerequisite. The particle-hole symmetry implicit in the effective Hamiltonian, which is experimentally observed in Ref. 1 and confirmed by the experimental data presented here, serves to constrain the shape of the phase boundary in the vicinity of the QCP. This is captured in the form of a refined power law (described below), and used in this work to more accurately extract an experimental estimate of the critical exponent ν.

In this paper, we present results of a set of experiments on $BaCuSi_2O_6$ down to 0.61 K from which we are able to extract critical scaling exponents describing the approach to the QCP. The experimental results are found to be consistent with the $\nu=2/3$ BEC critical exponent.

The proximity to the QCP is expected to be related to the ordering temperature (T_c) by a power law $T_c\sim(H-H_{c1})^\nu$,[11] which can be expressed in reduced form

$$t = f(h)(1-h)^\nu, \tag{1}$$

where $t=T_c/T_{max}$, $h=(H_{max}-H)/(H_{max}-H_{c1})$ (H_{max} and T_{max} represent the point on the phase boundary halfway between H_{c1} and H_{c2}, where H_{c2} is the field at which the magnetization saturates) and $f(h)_{h=1}$ is finite. The mean-field critical exponent $\nu=2/3$ is characteristic of the three-dimensional (3D) BEC universality class, and describes the scaling behavior of a 3D dilute interacting Bose gas near the QCP. The mean-field estimate is appropriate since the upper critical space dimension of 2 ($d_c=2$ because $z=2$ for this universality class) is exceeded.[9,12–14]

Magnetic torque, magnetocaloric effect, and specific heat measurements were performed to obtain points on the phase boundary into the ordered state. Features in these thermodynamic quantities characterize the classical 3D-*XY* phase transition into the ordered state at finite temperatures. Single crystal samples of $BaCuSi_2O_6$ grown by a flux-growth tech-

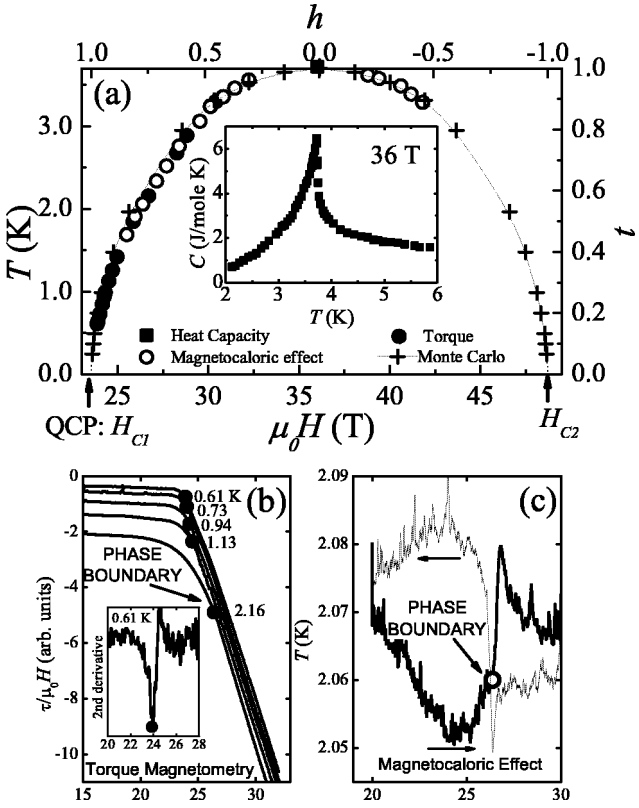

FIG. 1. (a) Points on the phase boundary are determined from magnetic torque (solid circles), magnetocaloric effect (open circles), specific heat (solid square) measurements and Monte Carlo simulation [+ symbols (the dotted line is a guide to the eye)]. The inset shows the lambda anomaly in specific heat measured at a magnetic field of 36 T. (b) Torque measured as a function of rising magnetic field at sample temperatures as indicated. The ordering transitions determined from a sharp feature in the second derivative (shown in the inset) are indicated on each of the torque curves. (c) Sample curve indicating the temperature change due to the magnetocaloric effect measured as a function of up and down sweeps in a magnetic field. The ordering transition is indicated on the curve.

nique were used for these experiments, whereas previous measurements on this material[1,2,10] used single crystals grown by a floating zone technique. Flux grown crystals were chosen because of a lower impurity content, a clearly defined Schottky anomaly in the zero field heat capacity, and narrower nuclear magnetic resonance lines.

The specific heat, measured at 36 T in a ^{4}He cryostat in the hybrid magnet at Tallahassee, is shown in the inset to Fig. 1(a), and shows the characteristic lambda anomaly indicating a second-order phase transition. The shape is identical to that in Ref. 1, which has been fit using directed-loop Monte Carlo simulations. The ordering temperature at 36 T is plotted on the phase diagram in Fig. 1(a).

Magnetic torque measurements to probe the ordering transition were performed in static magnetic fields up to 33 T in a ^{3}He fridge in Tallahassee. Samples were mounted on the moving plate of a capacitance cantilever, attached to a rigid plate rotatable about an axis parallel to the torque axis and perpendicular to the applied magnetic field. The sample is mounted with a small angle ($<10°$) between the applied field and the normal to the sample plane (easy axis $\hat{c}$), such that the applied field exerts a torque on the crystal due to the difference in g factor between the $\hat{a}$ and $\hat{c}$ orientations with $g_a \sim 2.053$ and $g_c \sim 2.303$.[15] The anisotropy in g results in an anisotropy in $H_{c1}=\Delta/g\mu_B$ (where Δ is the spin gap). Hence, on entering the magnetically ordered phase with increasing magnetic field, the anisotropy in magnetization causes a sudden increase in torque, as the field attempts to align the $\hat{c}$ axis more closely with the applied field. Torque was measured during field sweeps across the ordering transition at different temperatures.

The ordering transition is seen in field dependent torque curves in a temperature range 0.61–3.3 K [sample curves shown in Fig. 1(b)]. The field at which the phase transition occurs is obtained from a sharp feature in the second derivative of the torque [an example shown in the inset to Fig. 1(b)]. This is shown[16] using thermodynamic arguments to be the appropriate signature of the ordering transition, thus resolving the uncertainty in the literature over the correct technique.[3–7] The feature becomes weaker at higher temperatures, but can be extracted up to $T=3.3$ K. Examples of the ordering transitions thus obtained are indicated by solid symbols on the torque curves in Fig. 1(b). Points on the phase diagram obtained from torque measurements are shown as solid circles in the phase diagram in Fig. 1(a) (the experimental uncertainty is smaller than the symbol size.)

The magnetocaloric effect describes the temperature change of a magnetic material associated with an external magnetic field change in an adiabatic process. An abrupt change in the temperature with the changing magnetic field indicates a large field variation of the isothermal magnetic entropy, and is associated with an ordering transition. These measurements are a good probe of ordering transitions in a rapidly changing magnetic field.[17] Magnetocaloric effect measurements were performed in fields up to 45 T in a ^{4}He cryostat in the hybrid magnet in Tallahassee. Temperature changes are detected during magnetic field sweeps at different temperatures [shown in Fig. 1(c)]. The upturn in lattice temperature at H_{c1} (H_{c2}) in a rising (falling) field indicates a drop in magnetic entropy with ordering. Similarly, a dip in temperature in a falling (rising) field indicates the transition out of the ordered phase at $H_{c1}(H_{c2})$. The position of the ordering transition for $H<H_{\max}$ is obtained from the onset of the peak (as defined by the maximum in the first derivative) in a rising field and for $H>H_{\max}$ from the onset of the dip in a falling field. The ordering transition thus obtained for a representative field sweep is shown in Fig. 1(c). Points on the phase diagram obtained from magnetocaloric effect measurements are shown by open symbols in the phase diagram in Fig. 1(a).

Monte Carlo simulations for this system were performed using the directed-loop algorithm[18] [results are represented by + symbols in Fig. 1(a)]. Estimates of interdimer exchange coupling are refined from Ref. 1, with revised values of $J'=0.51$ meV and $J''=0.168$ meV yielding better agreement of the Monte Carlo simulations with experimental points on the phase diagram.

The particle-hole symmetry of the $BaCuSi_2O_6$ phase diagram enables us to extend the region near the QCP in which the power law can be fit. Equation (1) describes scaling near

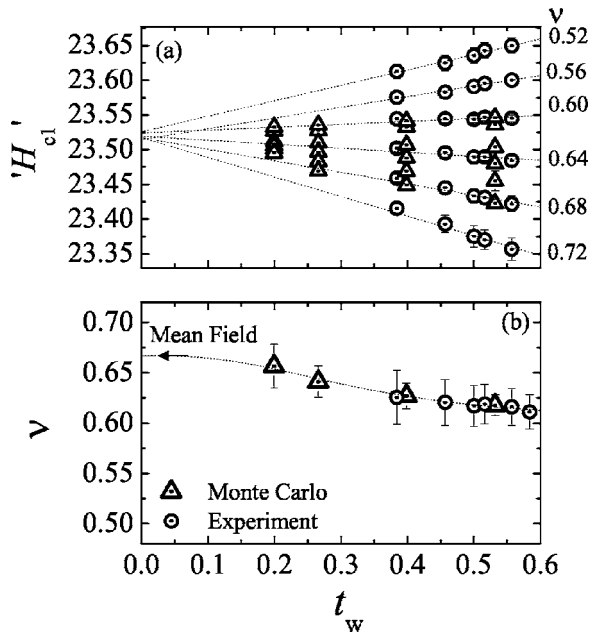

FIG. 2. (a) Circles represent estimates of 'H_{c1}' obtained from fitting the lowest few experimental points on the phase boundary in Fig. 1(c) in a window of increasing size t_w, to Eq. (2) for different fixed values of ν. The x axis t_w labels the highest reduced temperature of the fit window. The dotted lines show the linear convergence of 'H_{c1}' values at $t_w=0$. Triangles represent estimates of 'H_{c1}' similarly obtained from Monte Carlo simulation data for corresponding fixed values of ν, and similar convergence is observed. (b) Circles represent estimates of ν from fitting the lowest few experimental points on the phase boundary in Fig. 1(a) in a window of increasing size t_w, to Eq. (2) with $H_{c1}=23.52$ T determined from (a). The error bars are due to experimental uncertainty in determining values of H_c. Triangles represent estimates of ν from a similar fit to Monte Carlo simulation data. The dotted line is a guide to the eye, illustrating the approach of the Monte Carlo simulation to the mean field value as $t_w \to 0$.

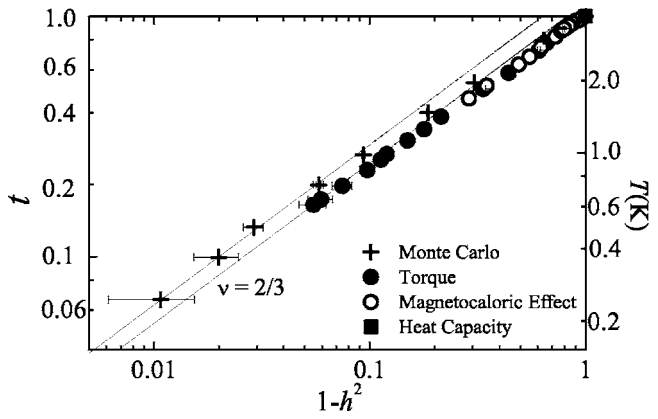

FIG. 3. Points on the phase boundary from magnetic torque (solid circles), magnetocaloric effect (open circles), and heat capacity (solid square) measurements for $H_{c1}=23.52$ T, $H_{max}=36.12$ T, $T_{max}=3.70$ K, and from Monte Carlo simulations (crosses). The lines represent Eq. (2) with $\nu=2/3$.

H_{c1} while $t \propto (1+h)^{\nu}$ describes scaling near H_{c2}. In other words, the particle-hole symmetry of the system implies that t is a function of h^2

$$t = g(h^2)[(1-h)(1+h)]^{\nu} \equiv g(h^2)(1-h^2)^{\nu}, \qquad (2)$$

where $g(h^2)$ varies more slowly than $f(h)$ near the QCP.

An additional improvement in the analysis presented here is an estimate of the universal region in which the power law can be extracted. We performed Monte Carlo simulations to identify the limit of the universal regime, and analyze data within this region to extract power-law behavior. Experimental limitations restrict the data available in the universal region to perform a two-parameter fit to ν and H_{c1} in Eq. (1). The analysis technique we report here to overcome this limitation is the independent determination of H_{c1} from the experimental data. This fixed value is used to perform a one-parameter fit to ν, which therefore requires a smaller number of data points in a limited range to obtain a statistically significant fit.

We use an empirical convergence approach to determine the best estimate of H_{c1}. Figure 2(a) shows the trend in the estimate of H_{c1} (denoted as 'H_{c1}') obtained by fitting the lowest few experimental points on the phase boundary in Fig. 1(a) in a window of increasing size t_w to Eq. (2) [where $g(h^2)$ is assumed to be constant to a first approximation] for different fixed values of ν. Near the QCP, it is empirically observed from linear extrapolation to $t_w=0$, that estimates of 'H_{c1}' become less dependent on ν, and converge to a single value irrespective of the value of ν [Fig. 2(a)]. Similar convergence to H_{c1} is observed for the Monte Carlo simulation results (with a narrower spread since simulations were run to lower temperatures than the experiments, thereby more tightly constraining the estimates of 'H_{c1}'.) The convergence is due to the fact that the QCP is at H_{c1}, independent of the path along which it is approached (characterized by ν). From this 'H_{c1}' convergence, we obtain an estimate of $H_{c1} \simeq 23.52 \pm 0.03$ T. This value of H_{c1} is then used to estimate the critical exponent ν.

The critical exponent ν is estimated from fitting Eq. (2) [with $g(h^2) \approx$ const.] to the narrowest temperature range near the QCP with a statistically significant number of experimental data points. Figure 2(b) shows the variation in ν with the size of the temperature window that is fit to Eq. (2) (points on the phase boundary are fit from the lowest value of $t=0.16$ to a highest value of $t=t_w$). We fit the lowest experimentally accessible temperature window containing nine data points down to 0.61 K to obtain a value of $\nu=0.63\pm0.03$. Performing a similar analysis on Monte Carlo simulation results reveals the expected increase in ν to the mean-field value as the temperature window is further reduced below currently accessible experimental temperatures [Fig. 2(b)]. The experimental estimate of $\nu=0.63\pm0.03$ based on measurements down to temperature $t=0.16$ is consistent with the theoretical mean field prediction of $\nu=2/3$ to within experimental error.

Figure 3 shows the comparison between the Monte Carlo simulation and the experimental data for $H_{c1}=23.52$ T. The lines represent the power law [Eq. (2)] with $\nu=2/3$. The universal region is indicated by the temperature range over which $\nu \to 2/3$ in the Monte Carlo simulation. A significant

number of experimental data points lie within this region, and we are able to obtain an experimental estimate of ν from the lowest statistically significant fit range ($t_w=0.38$) containing these data points (shown in Fig. 2). The Monte Carlo simulation and experimental data are in good agreement in the lowest experimentally accessible temperature window.

In summary, we performed magnetic torque and magnetocaloric effect experiments to map out the phase diagram in the vicinity of the QCP in the spin dimer system $BaCuSi_2O_6$. Points down to 0.61 K are fit to the power law $t=g(h^2)(1-h^2)^\nu$ [with $g(h^2)\approx$ const.] to give a value $\nu=0.63\pm0.03$, which is close to the theoretical value $\nu=2/3$. Experimental measurements of ν in the other prototypical spin dimer system $TlCuCl_3$ have resulted in lower values in the range 0.43–0.60.[3–7] However, the complexity of the $TlCuCl_3$ system in terms of an anisotropic lattice with multiple exchange constants, and a relatively large value of interdimer coupling relative to intradimer coupling makes that material more challenging to model. In addition, the presence of anisotropic crystal field effects that break rotational symmetry in $TlCuCl_3$ have been unambiguously demonstrated by high-field electron spin resonance (ESR) experiments.[19] Hence it has proved difficult to separate the physical origin of the deviation in ν from 2/3 in $TlCuCl_3$ from sources of error in the analysis technique. The other known experimental measurements of the BEC critical exponent ν have been on ^{4}He adsorbed in aerogel,[20–23] which is a realization of a dilute Bose gas, but is experimentally limited by the presence of a random external potential. $BaCuSi_2O_6$ is a unique U(1) symmetric spin dimer compound that enables experimental access to a QCP separating a quantum paramagnet from a Bose-Einstein condensate.[1] It provides an experimental realization of a BEC in a grand canonical ensemble in the absence of an external potential, with the region around the QCP accessible by a tuneable external magnetic field.

This work is supported by the National Science Foundation (NSF), Grant No. DMR-0134613. Experiments performed at the NHMFL were supported by the NSF, Florida State, and the Department of Energy. Monte Carlo computations presented here were performed with the SGI 2800/384 at the Supercomputer Center, Institute for Solid State Physics, University of Tokyo. The numerical work was supported by a Grant-in-Aid (Program No. 14540361) from Monkasho, Japan. S. E. S. thanks D. I. Santiago for helpful discussions. I. R. F. acknowledges support from the Alfred P. Sloan Foundation. S. E. S. acknowledges support from the Mustard Seed Foundation.

[1] M. Jaime, V. F. Correa, N. Harrison, C. D. Batista, N. Kawashima, Y. Kazuma, G. A. Jorge, R. Stern, I. Heinmaa, S. A. Zvyagin, Y. Sasago, and K. Uchinokura, Phys. Rev. Lett. **93**, 087203 (2004).

[2] Y. Sasago, K. Uchinokura, A. Zheludev, and G. Shirane, Phys. Rev. B **55**, 8357 (1997).

[3] T. Nikuni, M. Oshikawa, A. Oosawa, and H. Tanaka, Phys. Rev. Lett. **84**, 5868 (2000).

[4] Ch. Rüegg, N. Cavadini, A. Furrer, H.-U. Güdel, K. Krämer, H. Mutka, A. Wildes, K. Habicht and P. Vorderwisch, Nature (London) **423**, 62 (2003).

[5] H. Tanaka, A. Oosawa, T. Kato, H. Uekusa, Y. Ohashi, K. Kakurai, and A. Hoser, J. Phys. Soc. Jpn. **70**, 939 (2001).

[6] A. Oosawa, H. Aruga. Katori, and H. Tanaka, Phys. Rev. B **63**, 134416 (2001).

[7] Y. Shindo and H. Tanaka, J. Phys. Soc. Jpn. **73**, 2642 (2004).

[8] S. E. Sebastian, D. Yin, P. Tanedo, G. A. Jorge, N. Harrison, M. Jaime, Y. Mozharivskyj, G. Miller, J. Krzystek, S. A. Zvyagin, and I. R. Fisher, Phys. Rev. B **71**, 212405 (2005).

[9] T. Giamarchi and A. M. Tsvelik, Phys. Rev. B **59**, 11398 (1999).

[10] K. M. Sparta and G. Roth, Acta Crystallogr., Sect. B: Struct. Sci. **60**, 491 (2004).

[11] S. Sachdev, *Quantum Phase Transitions* (Cambridge University Press, Cambridge, 1999).

[12] M. P. A. Fisher, P. B. Weichman, G. Grinstein, and D. S. Fisher, Phys. Rev. B **40**, 546 (1989).

[13] N. Kawashima, J. Phys. Soc. Jpn. **73**, 3219 (2004).

[14] O. Nohadani, S. Wessel, B. Normand, and S. Haas, Phys. Rev. B **69**, 220402(R) (2004).

[15] S. E. Sebastian, P. Tanedo, Z. Islam, and I. R. Fisher (unpublished).

[16] The nonanalytic behavior of the free energy $F(T,H)$ is dominated by a single relevant exponent. Hence, the singular behavior of $F(T,B)$ when T and B are close to a critical point on the line $T_c(B)$ does not depend on the direction $u(H-H_c,T-T_c)$ of approach to the critical point, as long as it is not tangent to the critical line. In particular, for $u=T-T_c$ we have $\partial^2F/\partial^2u=C\propto u^{-\alpha}$. Choosing $u=H-H_c$, we obtain $\partial^2F/\partial^2H=\partial M/\partial H\propto(H-H_c)^{-\alpha}$. Since $\alpha\sim-0.015$ [M. Campostrini *et al.*, Phys. Rev. B **63**, 214503 (2001)] for a 3D *XY*-like transition, the second derivative of the magnetization is divergent at the critical point: $\partial^2M/\partial^2H\propto(H-H_c)^{-1-\alpha}$.

[17] M. Jaime, K. H. Kim, G. Jorge, S. McCall, and J. A. Mydosh, Phys. Rev. Lett. **89**, 287201 (2002).

[18] O. E. Syljuåsen and A. W. Sandvik, Phys. Rev. E **66**, 046701 (2002).

[19] V. N. Glazkov, A. I. Smirnov, H. Tanaka, and A. Oosawa, Phys. Rev. B **69**, 184410 (2004).

[20] B. C. Crooker, B. Hebral, E. N. Smith, Y. Takano, and J. D. Reppy, Phys. Rev. Lett. **51**, 666 (1983).

[21] P. A. Crowell, F. W. Van Keuls, and J. D. Reppy, Phys. Rev. B **55**, 12620 (1997).

[22] P. A. Crowell, F. W. Van Keuls, and J. D. Reppy, Phys. Rev. Lett. **75**, 1106 (1995).

[23] Tuning the particle hole density to provide access to the QCP requires absorption of ^{4}He in an external medium, which introduces a random external potential and effects due to surface absorption that influence system behavior.